Nonlinear flow in porous media

Sergio Rojas* and Joel Koplik
Benjamin Levich Institute and Department of Physics, City College of the City University of New York, New York, New York 10031
(Received 13 April 1998)

The flow of an incompressible liquid at nonzero Reynolds number Re in a two-dimensional model porous medium is studied via numerical simulation. The geometry is a random array of cylinders of square cross section and spectral element methods are used. We find a transition from linear Darcy flow at vanishing Re, to a cubic transitional regime at low Re, and then a quadratic Forchheimer when $\mathrm{Re}=O(1)$. In addition, some general remarks on scaling behavior and the form of the flow equation at finite Re are presented. [S1063-651X(98)13210-5]

PACS number(s): 47.55.Mh, 05.40.+j

I. INTRODUCTION

While the creeping flow of an incompressible viscous liquid in a porous medium is quite well understood, at least in principle [1], the situation at higher velocities has received rather less attention. At vanishing Reynolds number, the linearity of the underlying Stokes equations for fluid flow in the pore space makes it intuitively obvious that there should be a linear relation between average pressure gradient and flow rate, as exhibited in Darcy's law. Experiments and derivations of varying degrees of rigor are consistent with this reasoning and the only issue in such problems is the value of the proportionality constant, the permeability, and perhaps its relation to other transport coefficients. For flow at nonvanishing Reynolds number, experiments carried out by Forchheimer [2] and confirmed by others [3] indicate a quadratic dependence of pressure drop on flow rate, but the theoretical situation is far less clear.

The quadratic nature of the nonlinearity in the Navier-Stokes equations for the microscopic flow vaguely suggests that the average relationship should be quadratic as well, but a general and straightforward analytic derivation has not been found. A number of arguments appear in the literature, but all require some additional approximation. For example, volume averaging methods require closure assumptions [4], while in the earliest derivations based on matched asymptotic expansions [5] further phenomenological assumptions are needed and are restricted to the high porosity limit [6]. Alternatively, there are heuristic scaling arguments (see below) or approximate arguments based on the Oseen approximation [7]. A systematic multiple scale analysis based on the smallness of the characteristic size of the porous medium microstructure relative to typical macroscopic lengths correctly reproduces Darcy's law in creeping flow [9], but gives a *cubic* law at small but nonzero Reynolds number [8]. The latter is generally not found experimentally (but see [10]). Recent numerical simulations have clarified the situation considerably; several calculations of flow past arrays of circular cylinders find a transitional cubic relation at small Reynolds number, followed by a quadratic law at larger values [11,12,7].

In this paper we will present further numerical confirmation in a different geometry of the two-stage transition scenario just described: a pressure drop vs flow rate relation varying from linear to cubic to quadratic as the Reynolds number increases. In addition, a variety of remarks and arguments on this problem, relating to the form of the averaged equation and the relation between permeability and conductivity, will be made. In Sec. II, we define the variables and scaling operations and discuss the form of the macroscopic relation between averaged pressure gradient and velocity. Section III describes the numerical computations, based on a spectral element method applied to a random array of cylinders of square cross section. In Sec. IV we discuss the numerical results. Concluding remarks appear in Sec. V.

II. EFFECTIVE FLOW EQUATION

We consider a steady incompressible Newtonian fluid of density ρ and viscosity μ flowing at finite Reynolds number in a fixed porous medium, with equations of motion

$$\rho\mathbf{u}\cdot\nabla\mathbf{u}=-\nabla p+\mu\nabla^2\mathbf{u},\quad \nabla\cdot\mathbf{u}=0 \tag{1}$$

and no-slip boundary conditions on the surface of the pore space. The latter will be modeled as a fixed array of ''grains,'' particles of typical size a making up the solid matrix. Ultimately we will suppose that the porous medium occupies the central section of a slab (two dimensions) or tube (three dimensions), with free fluid regions upstream and downstream, so that the asymptotic flow at a large distance from the porous medium is Poiseuille. The relevant velocity scale U is the average velocity in the free fluid regions (or, equivalently, ϕ times the average velocity in the porous medium, where ϕ is the porosity) and a suitable length scale for flow within the pore space is the square root of the permeability k, so we define the Reynolds number as

$$\mathrm{Re}=\frac{\rho U k^{1/2}}{\mu}. \tag{2}$$

*Present address: Intevep, SA Apartado 76343, Caracas 1070A, Venezuela.

The value of Re controls the importance of nonlinear inertial corrections to the microscopic equations in the pore space and when $\mathrm{Re}=O(1)$ we expect a nonlinear macroscopic equation.

At vanishing values of Re, the averaged pressure (P) and velocity (U) satisfy Darcy's law

$$\nabla P = -\frac{\mu}{k}\mathbf{U}, \tag{3}$$

where the averaging is either spatial, over regions of space containing many grains, or statistical, over an ensemble of porous media with the same distribution of grains. We have assumed in writing this formula that the porous medium is statistically homogeneous and isotropic, so there is preferred orientation and k does not vary spatially. At finite values of Re, rotational invariance constrains the more general averaged equation to the form

$$\nabla P = -\frac{\mu}{k}\mathbf{U}[1+f(\mathrm{Re})], \tag{4}$$

in which the *a priori* unknown function f is the focus of interest.

Note that we have not included in Eq. (4) a possible convective derivative term of the form $\rho\mathbf{U}\cdot\nabla\mathbf{U}$, which is allowed by rotational invariance and occasionally included in porous medium modeling studies. Such a term would not appear in any flow that is one dimensional on average, since then the average velocity cannot vary, but might appear if the flow is allowed to vary on some length scale L much larger than $k^{1/2}$ or the grain scale a. The reason for omitting the convective derivative is that a simple scaling estimate implies that such a term will be macroscopically negligible [13]. It is convenient in this context to nondimensionalize Eq. (4) using a velocity scale U_0, the length scale L, and a Darcy pressure scale $\mu U_0/k$. The dimensionless form of Eq. (4) plus the convective derivative term then becomes

$$\nabla P = -\mathbf{U}[1+f(\mathrm{Re})] - \frac{\rho U_0 k}{\mu L}\mathbf{U}\cdot\nabla\mathbf{U}$$

and the coefficient of the last term is Re times the small number $k^{1/2}/L$. In fact, for purposes of macroscopic flow, it is more sensible to work in terms of a *macroscopic* Reynolds number $\mathcal{R}=\rho UL/\mu$, in which case the coefficient of the possible convective derivative term is $\mathcal{R}(k/L^2)$ and quite negligible in most circumstances.

The form of the correction $f(\mathrm{Re})$ to Darcy's law has been a matter of controversy, which has clarified considerably recently. If one assumes, following Mei and Auriault [8], that for finite but small Reynolds number there is a regular perturbation expansion in powers of velocity and the small parameter $\epsilon=k^{1/2}/L$, then rotational invariance essentially dictates a cubic correction. (The original derivation assumed an additional relation between ϵ and Re, but it is straightforward to show that the result holds more generally [14]. Alternatively, arguments based on fore-aft symmetry [7,10] yield the same result.) In fact, the quadratic Forchheimer equation circumvents this difficulty on the one hand by a nonanalytic dependence on the absolute value of the velocity through Re and on the other by breaking fore-aft symmetry in a finite-Re wake.

A heuristic argument for a quadratic correction to Darcy's law [$f(\mathrm{Re})\sim\mathrm{Re}$] at high Re can be obtained by a boundary-layer-like scaling argument, if one assumes that at finite Re the microscopic flow field in a disordered porous medium does not have a preferred spatial direction for its most rapid variation. In a random porous medium, one expects the flow to ''wrap around'' the grains, in a fully three-dimensional fashion. The most rapid variation in the velocity would occur in a direction locally normal to the grains in a thin boundary layer and therefore without a strong bias with respect to the average flow. This assertion is in distinction to the common boundary-layer picture, say for flow along a flat plate [15], where there are distinct directions for the average flow and the most rapid variation. In the spirit of the derivation of boundary layer equations, if we estimate the derivatives in Eq. (1) by a typical magnitude divided by a typical length scale of variation, we have

$$\rho\frac{U^2}{\Delta_L}\sim\frac{P}{\Delta_L}+\mu\left[\frac{U}{\Delta_L^2}+\frac{U}{\Delta_T^2}\right],$$

where L,T refer to longitudinal and transverse length scales, respectively. If we assume that $\Delta_L\sim\Delta_T$ and that the pressure variations are negligible, then $\Delta\sim\mu/\rho U$. Alternatively, if the pressure has an inertial scaling $P\sim\rho U^2$ the same result follows, while if the pressure has a Darcy scaling $P\sim\mu U/k$ this term would be negligible when the velocity is high enough to make the boundary layer thin compared to $k^{1/2}$, the typical radius of the narrowest parts of the flow paths controlling the permeability. Given this boundary layer scaling, we can determine the overall pressure drop $\mathcal{P}$ across the porous medium by use of the exact expression [16] for energy dissipation,

$$Q\mathcal{P}=\mu\int d\mathbf{x}\sum_{i,j}\left(\frac{\partial u_i}{\partial x_j}\right)^2,$$

where the integral runs over the pore space. The right-hand side is estimated as the grain surface area times the boundary layer thickness Δ times the square of the largest velocity gradient U/Δ, giving $U\mathcal{P}\sim\Delta(U/\Delta)^2$ or $\mathcal{P}\sim U^2$.

III. SIMULATION METHOD

We wish to compute the flow in a class of model porous media, composed of a two-dimensional regular or random arrays of fixed square obstacles placed in the interior of a channel. Examples are shown in Fig. 1, in which the first is strictly periodic, while the others have obstacles centered at random positions with successively decreasing size, so as to generate a sequence of increasing porosities. The properties of the various cases considered are summarized in Table I. Figures for all cases and further details on the numerical simulations may be found in [17]. In the figures, the upper and lower horizontal lines represent the confining walls of the channel and the open regions to either side represent empty sections of straight channel in which a Poiseuille velocity profile may be assumed. The obstacles are idealiza-

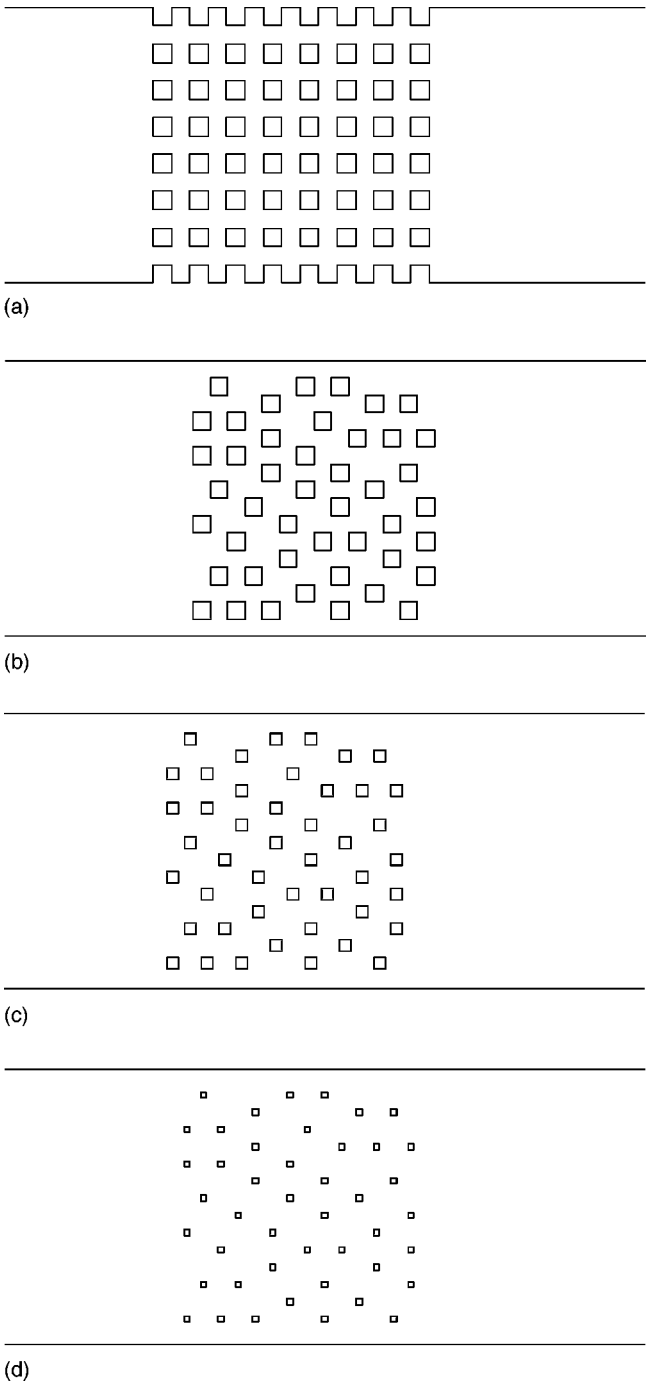

FIG. 1. Examples of the porous media geometries studied numerically in this work.

tions of the solid grains found in laboratory and field systems and the overall configuration models a ''core'' of porous material placed in a jacketing container.

These geometries have been chosen for computational convenience and are evidently highly idealized models of realistic naturally occurring porous media, but we believe that the differences are not relevant to our conclusions. First, we are working with systems in two dimensions rather than three or, alternatively, flow at right angles to the axes of an array of cylinders of a square cross section. While many physical phenomena exhibit a distinction between two and three dimensions, there is no reason to expect a problem for the laminar flow of a single viscous liquid in a well-connected pore space. The two- and three-dimensional experiments cited above at various Reynolds numbers do not show a difference in qualitative behavior, and likewise all of the theoretical arguments mentioned do not have any dimensional sensitivity. Only if the connectivity of the pore space were an issue, as would occur in immiscible displacement or in the percolation limit for the single-fluid flows studied here, is dimension likely to matter. Second, we have square grains oriented with sides exactly parallel to the average flow. However, the precise shape is unlikely to be qualitatively significant because there will always be a viscous skin region surrounding any solid body, which effectively rounds the corners (see below for a quantitative discussion) and the flow around the most upstream grains will have the effect of randomizing the direction of the streamlines incident on those downstream. Furthermore, one can think of the squares as including the sharp corners sometimes found on grains in geological systems and absent when the grains are commonly modeled as circles or spheres. Finally, one might object that our systems are rather small, containing only 40–60 grains, and all have relatively high porosity. We certainly expect that the numerical value of coefficients such as the permeability to differ from those in more compact systems, but this is not the focus of this work. We are concerned with the general form of the flow equation and it is reasonable to expect that the essence of the system is one with a rapid local variation in the flow field imposed by an irregular internal bounding surface. In fact, flow in rough pipes exhibits an analogous transition from linear to quadratic drag [15].

TABLE I. Geometric parameters and computational results for various geometries. Systems 1 and 2 are quasiperiodic [2 is displayed in Fig. 1(a)] and the others are random [3, 6, and 8 are shown in Figs. 1(b), 1(c), and 1(d), respectively]. The length scale for the ''grain size'' a and the permeability k is the width of the channel, while the conductivity is normalized to the pure-fluid value. Numbers in square brackets denote multiplicative powers of 10.

System	ϕ	a	k	σ	B	C
1	0.762	0.0625	1.79[-4]	0.566	0.170	0.063
2[a]	0.716	0.0666	2.00[-4]	0.522	0.0327	0.0206
3[b]	0.842	0.0625	3.29[-4]	0.677	0.101	0.0481
4	0.884	0.05	5.51[-4]	0.781	0.090	0.0377
5	0.901	0.0469	6.22[-4]	0.804	0.0871	0.0349
6[c]	0.922	0.0416	7.56[-4]	0.842	0.0824	0.0328
7	0.956	0.0312	1.10[-3]	0.908	0.0742	0.0241
8[d]	0.980	0.0208	1.62[-3]	0.958	0.0619	0.0241
9	0.993	0.0125	2.25[-3]	0.984	0.0505	0.018

The numerical method used is a spectral finite element method, encoded in the commercial software package NEKTON [18]. The flow domain is divided into trapezoidal elements and the flow fields are expanded into polynomials of a specified order within each element. As an example of the element decomposition, the model porous medium shown in Fig. 1(d) is decomposed in Fig. 2. The calculations are carried out, typically with fifth-order polynomials to start, and then refined to order 7 or 9 as a test of the accuracy of the computation. The resulting variation in the pressure difference is less than 1%, over the full range of Reynolds

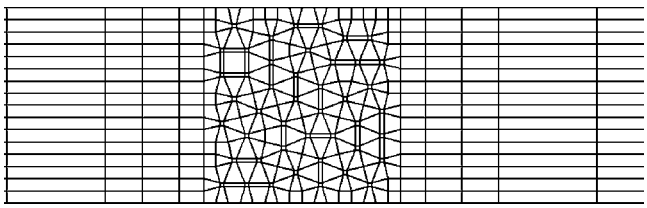

FIG. 2. Computational mesh corresponding to Fig. 1(d).

numbers studied. Alternately, the calculation could be refined by subdividing the elements into smaller ones, but the memory requirements made this option impractical.

The idea of the calculation is to specify the average velocity U through the Poiseuille profile at the sample ends, $u(y)=6Uy(w-y)/w^2$, where w is the channel width, and compute the net pressure drop from end to end using NEKTON. To focus on the porous media part, we subtract off the (Poiseuille) pressure drops in the empty regions between the ends and the grain-filled region,

$$\Delta P_{\mathrm{PM}}=(P_1-P_2)-12\mu U(x_2-x_1-L_{\mathrm{PM}})/w^2, \qquad (5)$$

where $P_{1,2}$ are the upstream and downstream pressures measured at the points $x_{1,2}$ and L_{PM} is the length of the central porous segment. We then fit the resulting porous medium pressure drop to an appropriate polynomial in U,

$$-\nabla P\equiv\frac{\Delta P_{\mathrm{PM}}}{L_{\mathrm{PM}}}=\frac{\mu}{k}U+\frac{B\rho}{k^{1/2}}U^2+\frac{C\rho^2}{\mu}U^3, \qquad (6)$$

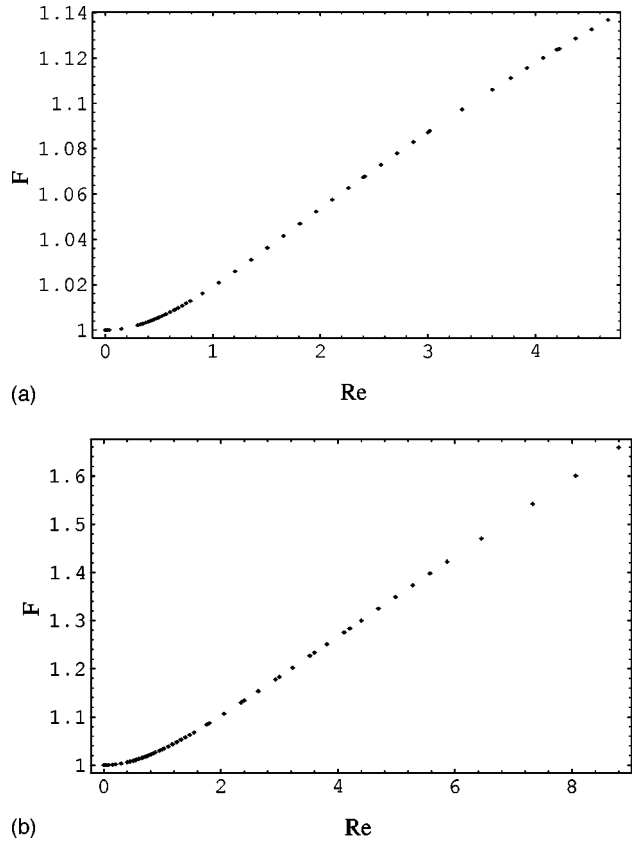

FIG. 3. Variation of the normalized pressure drop F with Re, for (a) system 2 shown in Fig. 1(a) and (b) system 9 shown in Fig. 1(d).

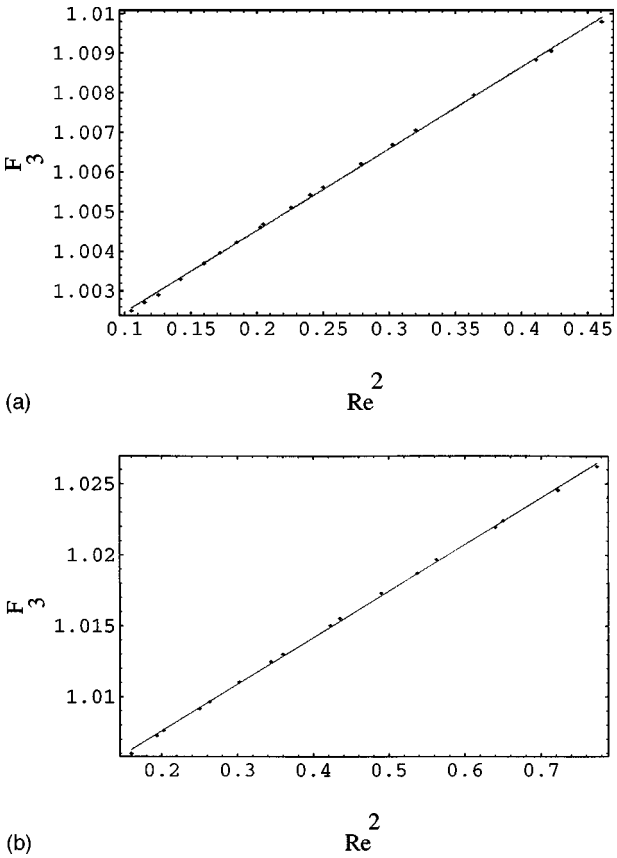

FIG. 4. Quadratic variation of F with Re in the transitional regime, corresponding to Fig. 3.

where the coefficients B and C are dimensionless. We have anticipated that the pressure gradient will involve at most cubic terms and the notation is similar to that of Beavers and Sparrow [3], whose experimental geometry resembles ours. It is convenient to recast the latter equation into fully dimensionless form, using the Reynolds number given in Eq. (2), by defining a dimensionless pressure gradient normalized to Darcy flow,

$$F\equiv\frac{k}{\mu U}\frac{\Delta P_{\mathrm{PM}}}{L_{\mathrm{PM}}}=1+B\,\mathrm{Re}+C\,\mathrm{Re}^2. \qquad (7)$$

Aside from global fits using Eq. (7), we will also consider piecewise fits to the transitional cubic and high-Re quadratic regions and it is convenient to have the special cases

$$F_2=1+B\,\mathrm{Re}, \qquad (8a)$$

$$F_3=1+C\,\mathrm{Re}^2. \qquad (8b)$$

For each geometry, we first solve the Stokes equations to find the permeability, defined operationally by dropping the nonlinear terms in Eq. (6), and then the full (steady, incompressible) Navier-Stokes equations to study nonlinear effects. The boundary conditions on the calculations are a no-slip velocity on edges of each grain and on the sides of the channel and a Poiseuille velocity profile at the left and right boundaries. Although the systems studied are not fully rotationally invariant, we have made an effort to choose geometries having at least a discrete 90° rotational invariance. In

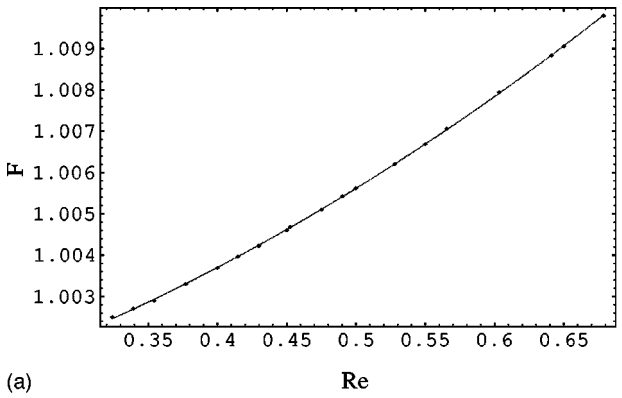

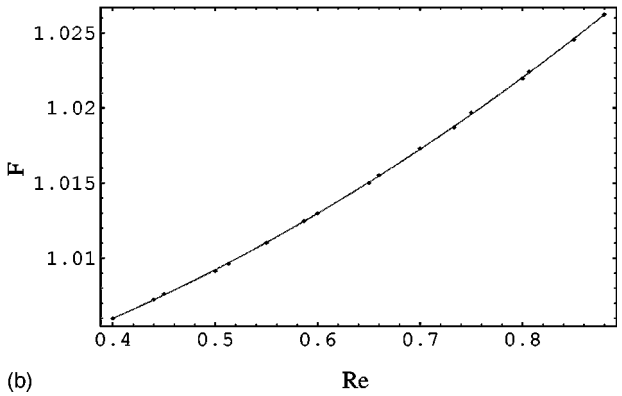

FIG. 5. Combined linear plus quadratic fit to a larger transition region, as in Fig. 3.

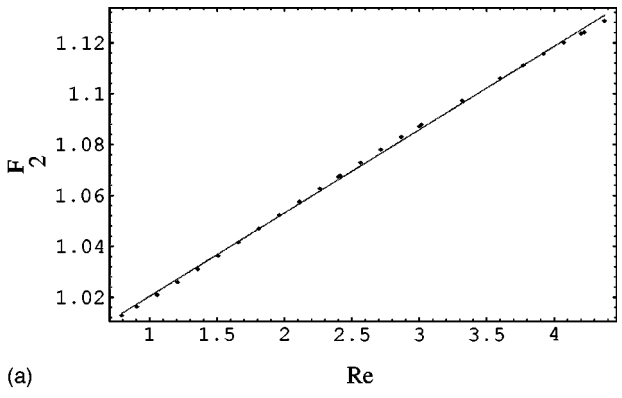

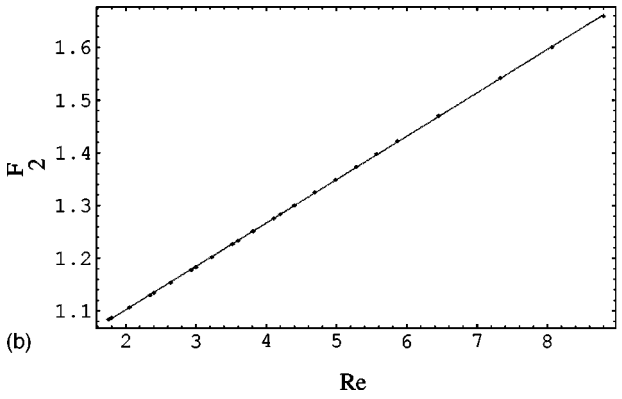

FIG. 6. Variation of F with Re for Re>1, as in Fig. 3.

fact, we find that when the grain-filled region is rotated by 90°, the change in permeability is less than 3%.

IV. NUMERICAL RESULTS

We have calculated the pressure drop as a function of Reynolds number for the systems listed in Table I and illustrated in part in Fig. 1. All regular geometries and all random geometries have essentially the same behavior, respectively, so it suffices to discuss one example of each in detail. The variation of the dimensionless pressure drop with Re is shown in Figs. 3(a) and 3(b) for one typical periodic case and one typical random case, corresponding to systems 2 [Fig. 1(a)] and 8 [Fig. 1(d)] in Table I. As stated above, the numerical results are Darcy flow at small Re (constant F), a cubic transitional (quadratic F) regime at Re$=0.2$–1, and a quadratic behavior (linear F) at higher Re. To verify these statements in more detail, we first focus on the transitional regime in Figs. 4(a), 4(b), indicating how a linear dependence of F_3 vs Re^2 fits the data reasonably well. Of course, allowing for a more complicated behavior with an additional parameter provides an improved fit and we see in Figs. 5(a) and 5(b), that both better agreement and an extended range of Re values are provided by retaining linear and quadratic terms in F. The corresponding coefficients are recorded in Table I. The values of B are qualitatively consistent with the experiments of Beavers and Sparrow on flow past arrays of circular cylinders, who found a value 0.074 for the corresponding parameter. At Re>1, as indicated in Figs. 6(a) and 6(b) however, the simulation results do not show any quadratic behavior at all.

In addition to these finite-Re considerations, it is of interest to consider the variation of conductivity and permeability with porosity in the porous media studied here. For conductivity, we imagine that fluid in the pore space has an electrical conductivity σ_0, impose voltages 1 and 0 on the left and right edges of the sample, respectively, and compute the net current flow I. The voltage drop in the pure-fluid regions is subtracted analogously to the pressure subtraction in Eq. (5) and the relative conductivity of the porous medium is defined as

$$g=\frac{1}{\sigma_0}\frac{I/w}{\Delta V/L_{\mathrm{PM}}}. \tag{9}$$

(For the calculation, we use NEKTON to solve the mathematically isomorphic heat flow problem.) The variation of g with

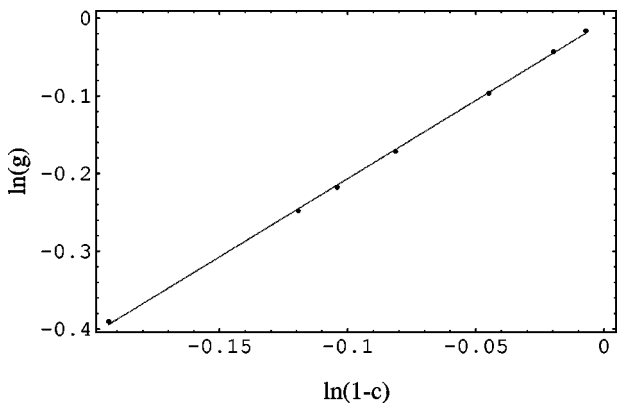

FIG. 7. Variation of effective conductivity with solid fraction ($c=1-\phi$) for the random systems 3–9.

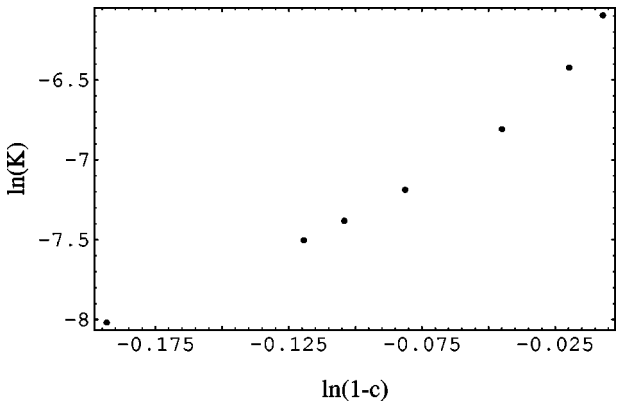

FIG. 8. Variation of normalized permeability ($K=k/w^2$) with solid fraction for the random systems 3–9.

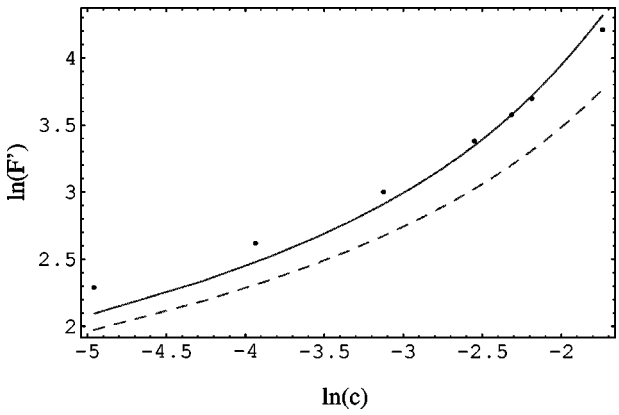

FIG. 9. Normalized drag vs solid fraction for the random systems 3–9. The points are the numerical data, the dashed curve is Eq. (10) using the actual grain cross sectional area and solid fraction and the solid line is Eq. (10) with an ″effective″ grain area 1.5 times larger.

porosity (equivalently, one minus the solid concentration c) is shown in a log-log plot in Fig. 7. The fit is $g\sim\phi^2$, a dependence often found in porous media [1], although various values of the exponent are common. Similarly, the variation of permeability (normalized to the channel-width squared) with porosity is shown in Fig. 8, but this does not appear to follow a power law. Although for some porous media and in some theoretical models there are interrelated power-laws for g and K, such a relation is not always observed in the laboratory. For example, the ''shrinking tube'' model of Wong *et al.* [19], motivated by experiments on a compact porous medium of well-fused glass beads, predicts a permeability exponent twice the conductivity exponent, but in the geometry considered here the porosity variation would not be accurately described in these terms.

Alternatively we can compare the permeability variation with porosity to calculations of the drag on an array of circular cylinders by Sangani and Acrivos [20]. These authors find that a normalized drag per unit length of cylinder $F'=A/ck$ (A is the cross sectional area and c is the solid fraction) can be expressed as

$$F'=\frac{4\pi}{-\frac{1}{2}\ln c-0.738+c-0.887c^2+2.039c^3}. \qquad (10)$$

Now for the *regular* square array in Fig. 1(a), the simulational result for F' is 4.36, while Eq. (10) gives 4.43. The discrepancy may be rationalized based on the familiar Stokes's flow theorem that the drag on a solid particle is greater than the drag on any smaller particle that is geometrically contained within it [21,16]. Here our square grains would contain the inscribed circular grains of radius $a/2$ and are themselves contained within circumscribing circles of radius $a/\sqrt{2}$. Formula (10) gives lower and upper bounds for F' of 4.08 and 4.72, respectively, which indeed bracket the numerical value.

In the random case, we plot F' using our results for k vs c, using the actual cross sectional area of the grains, as the points in Fig. 9. The dashed curve is Eq. (10), which has a similar shape but differs by a multiplicative factor of about 0.715. In this case, the resulting drag is *larger* than the ostensible upper bound derived from Eq. (10) and circumscribing circles. The qualitative reason is that for a given set of obstacles, random systems are less permeable than regular ones. The permeability is controlled by the narrowest spanning set of flow paths, and a random array will have some narrower gaps [22]. Alternatively (in a manner similar to [7]), we can adjust the value of grain cross sectional area by a multiplicative factor 1.5 to obtain the solid curve in the figure, arguing that a random array of square grains should be equivalent to a regular array of circular grains at a suitably higher concentration.

V. CONCLUSIONS

We have discussed several aspects of finite Reynolds number flow in a model porous medium. The overall result is that the pressure drop in a flow that is on average unidirectional is linear as $\mathrm{Re}\to 0$, quadratic at finite Re, and has a cubic dependence in the transitional region. These conclusions are in agreement with most (but not all) previous theoretical, computational, and experimental studies, but we have examined a somewhat different geometry and thereby helped establish their robustness. In addition, we have provided heuristic arguments for the behavior (4) for general flows, as well as some justification for quadratic drag. A number of open questions remain, most notably to obtain some insight into the numerical value of the coefficient B and perhaps to relate it to other porous media transport coefficients. A first-principles derivation of the quadratic drag law for random systems might help address this question and would certainly be of conceptual interest in general.

ACKNOWLEDGMENTS

We thank A. Acrivos and R. Mauri for helpful discussions. This research was supported by Intevep, SA, and the U.S. Department of Energy.

[1] J. Bear, *Dynamics of Fluids in Porous Media* (Elsevier, Amsterdam, 1972); A. E. Scheidegger, *The Physics of Flow in Porous Media*, 3rd ed. (University of Toronto Press, Toronto, 1974); F. A. L. Dullien, *Porous Media: Fluid Transport and Pore Structure*, 2nd ed. (Academic, New York, 1992).

[2] P. Forchheimer, *Hydraulik*, 3rd ed. (Teubner, Berlin, 1930), and original references therein.

[3] G. S. Beavers and E. M. Sparrow, J. Appl. Mech. **36**, 711 (1969); G. S. Beavers, E. M. Sparrow, and D. E. Rodentz, *ibid.* **40**, 655 (1973); S. Ergun, Chem. Eng. Prog. **48**, 89 (1952); K. Yamamoto and Z. Yoshida, J. Phys. Soc. Jpn. **37**, 774 (1974); A. Dybbs and R. V. Edwards, in *Fundamentals of Transport Processes in Porous Media*, edited by J. Bear and M. Y. Corapcioglu (Nijhoff, Dordrecht, 1984); R. M. Fand, B. Y. K. Kim, A. C. C. Lam, and R. T. Phan, J. Fluids Eng. **109**, 268 (1987).

[4] H. Ma and D. W. Ruth, Transp. Porous Media **13**, 139 (1993); S. Whittaker, *ibid.* **25**, 27 (1996).

[5] Y. Kaneda, J. Fluid Mech. **167**, 455 (1986).

[6] H. Cheng and G. Papanicolaou, J. Fluid Mech. **335**, 189 (1997).

[7] D. R. Koch and A. J. C. Ladd, J. Fluid Mech. **349**, 31 (1997).

[8] C. C. Mei and J.-L. Auriault, J. Fluid Mech. **222**, 647 (1991).

[9] J. B. Keller, in *Nonlinear P.D.E.s in Engineering and Applied Science*, edited by R. L. Sternberg *et al.* (Dekker, New York, 1980); J. Rubenstein and S. Torquato, J. Fluid Mech. **206**, 25 (1989).

[10] M. Firdaouss, J.-L. Guermond, and P. Le Quéré, J. Fluid Mech. **343**, 331 (1997).

[11] D. A. Edwards, M. Shapiro, P. Bar-Yoseph, and M. Shapira, Phys. Fluids **2**, 45 (1990).

[12] D. R. Noble, J. G. Georgiadis, and R. O. Buckius (unpublished).

[13] This result was pointed out to us by A. Acrivos, based on a slightly different argument.

[14] J. Koplik and R. Mauri (unpublished).

[15] H. Schlichting, *Boundary Layer Theory*, 6th ed. (McGraw-Hill, New York, 1968).

[16] S. Kim and S. J. Karrila, *Microhydrodynamics* (Butterworths, Boston, 1991).

[17] S. Rojas, Ph.D. dissertation, City University of New York, 1998 (unpublished).

[18] NEKTON, available from Fluent Inc., 10 Cavendish Court, Lebanon, NH 03766.

[19] P.-z. Wong, J. Koplik, and J. P. Tomanic, Phys. Rev. B **30**, 6606 (1984).

[20] A. S. Sangani and A. Acrivos, Int. J. Multiphase Flow **8**, 343 (1982).

[21] R. Hill and G. Power, Q. J. Mech. Appl. Math. **9**, 313 (1956).

[22] Another analogy is to resistor networks: If the resistors are all in parallel, a random distribution of resistors has the same total resistance if each is replaced by the average value, whereas if the resistors are in series, the total resistance of the random systems is dominated by the largest individual value. An interconnected two-dimensional network lies in between these two extremes.